Bull. Math. Soc. Sc. Math. Roumanie
Tome 48(96) No. 2, 2005, 119–137

An efficient algorithm to solve large non linear elastodynamic problems with contact and friction

by
Mikael Barboteu

Abstract

In this work, we present the combination of two efficient algorithms to solve non linear elastodynamic problems with a large number of degrees of freedom. The non linearities come from hyperelastic constitutive law but also from frictional contact conditions. These large non linear problems are generally charaterized by large computational times. So initialy, we focus our attention on the development of a time-stepping scheme which makes it possible to have energy conservation properties and also to reduce the time integration cost; we present then an energy-conserving algorithm for hyper-elastodynamic contact problems which differs from the usual approaches. The second improvment deals with the solution of the linearized problems; in order to reduce the cost of this stage, we present a scalable domain decomposition method well adapted to solve the corresponding linearized systems.

Key Words: Non linear dynamics, Large deformations, Frictional contact, Energy conserving algorithm, Domain decomposition method, Balancing method, Numerical scalability.
2000 Mathematics Subject Classification: Primary: 65K05, 74H15, 74B20, 74M20, 65Y05, 65N99, Secondary: 74M15, 74M10, 49M15, 68W10, 65N22.

1 Introduction

Non linear elastodynamic problems with a large number of degrees of freedom necessitate the use of efficient and robust algorithms in order to reduce the solution cost and also to have some energy conservation properties. In a general way, the solution of such problems is realized by coupling a time integration algorithm to deal with the dynamic part and a linear iteration algorithm to treat the non linearities. In this work, we investigate these two subjects with an aim of performing the integration scheme and with an aim of reducing the solution cost

of linearized systems by using a domain decomposition method. These investigations are carried out in order to propose algorithmic adaptations well suited to hyperelastodynamic problems with contact and friction.

Firstly in section 2, we present a new energy-conserving algorithm for impact problems which differs from the usual approaches ([13] and [9]). During the last years, the construction of energy conserving time integration methods to solve nonlinear elastodynamic problems has attracted the interest of many researchers ([20, 8, 5] ...). Furthermore, many works have been devoted to extend these conservative formulations to frictionless impact; more precisely, Laursen and Chawla [13] and Amero and Petocz [4] have shown the interest of the persistency condition to conserve the energy in the discrete framework. But these contributions concede a contact interpenetration which vanishing as the time step tends towards zero. Recently, this drawback is resolved by Laursen and Love [14] by introducing a discrete jump in velocity and by Hauret [9] by considering a specific penalized enforcement of the contact conditions. The approach presented in this work permits to ensure both the Kuhn-Tucker and persistency conditions at the end of each time step. These two laws are enforced during each time increment by using an extended Newton method. In section 2.1, we recall some general aspects of non linear elastodynamic problems with contact and friction. The section 2.2 permits also to recall the usual energy conserving frameworks used to solve non linear elastodynamic problems. In section 2.3, we present a new energy-conserving algorithm to treat impact problems. In the last section 2.4 of the first part, representative numerical simulations are presented to assess the performance and also to underscore the conservative behaviour of the proposed method.

The second part of this work (section 3) is devoted to present a scalable domain decomposition method to solve dynamic frictional contact problems in large deformations. The solution of this kind of problems by standard algorithms generates strongly non symmetric and ill-conditionned systems. So, large non linear elastodynamic problems represent an appropriate application field for substructuring methods which are efficient on parallel computer with the proviso of using specific preconditioner techniques well adapted to the mechanical modeling. According to the reasons mentioned above and in order to overcome these difficulties, we develop an adapted Balancing domain decomposition method [18, 15] appropriated to solve this kind of systems. By using the theoretical framework of Schwarz additive decomposition method [15, 17], we propose a two level Neumann-Neumann preconditioner (Balancing method) based on the construction of a coarse space of "lower energy" modes adapted to finite deformations problems with dynamic process. With such problems, some rigid body motions cannot be detected in the factorization step of the local tangent matrices of subdomains. So we have to make some adaptations for taking into account all lower energy modes. In section 3.1, basic scalable domain decomposition approaches are presented. The section 3.2 is devoted to the adaptations of the two level Neumann-Neumann preconditioner. In last section 3.3, we test the efficiency of this updated Balanc-

ing domain decomposition method on numerical solutions of non linear dynamic problems presented in section 2.4.

2 A new energy conserving method

2.1 Non linear elastodynamic problems

Dynamic deformable body systems in large deformations are governed by non linear time dependent equations. In this work, we consider non linear elastic behaviours which are characterized by hyperelastic constitutive laws. The first Piola-Kirchoff tensor $\mathbf{\Pi}$ is given by the relation $\mathbf{\Pi} = \partial_{\mathbf{F}} W(\mathbf{F})$ where $W(\mathbf{F})$ is the internal hyperelastic energy and $\mathbf{F}$ is the deformation gradient defined by $\mathbf{F} = \mathbf{I} + \nabla \mathbf{u}$ ($\mathbf{u}$ represents the displacement vector). A typical non linear elastodynamic problem defined in a reference configuration can be governed by the following variational form,

$$\begin{cases} \text{Find } \mathbf{u} \in L^2(]0;T[;U_0) \quad \text{such that for each } t \in]0;T[, \\ \int_\Omega \rho \ddot{\mathbf{u}}(t).\mathbf{v} + \int_\Omega \mathbf{\Pi}(t) : \nabla \mathbf{v} - \int_\Omega \mathbf{f}(t).\mathbf{v} - \int_{\partial_g \Omega} \mathbf{g}(t).\mathbf{v} = 0, \quad \forall \mathbf{v} \in U_0 \\ \frac{\partial^2 \mathbf{u}(t)}{\partial t^2} = \ddot{\mathbf{u}}(t) \quad \text{in } U_0 \end{cases} \tag{1}$$

where ρ denotes the mass density; $\mathbf{f}$ and $\mathbf{g}$ are the external force densities. A dot superscript indicates the time derivative. The set $U_0 = \{\mathbf{v} \in H^1(\Omega)^{dim}; \mathbf{v} = \mathbf{0} \text{ on } \partial_0 \Omega\}$ represents the space of kinematically admissible displacement fields. In the case we consider frictional contact conditions on the surface contact $\partial_c \Omega$, the variational form of the non linear elastodynamic problem can be written as follows,

$$\begin{cases} \text{Find } \mathbf{u} \in L^2(]0;T[;U_0) \quad \text{such that for each } t \in]0;T[, \\ \int_\Omega \rho \ddot{\mathbf{u}}(t).\mathbf{v} + \int_\Omega \mathbf{\Pi}(t) : \nabla \mathbf{v} - \int_\Omega \mathbf{f}(t).\mathbf{v} - \int_{\partial_g \Omega} \mathbf{g}(t).\mathbf{v} + \mathcal{P}_{c+f}(t) = 0, \quad \forall \mathbf{v} \in U_0, \end{cases} \tag{2}$$

where the frictional contact term is given by

$$\mathcal{P}_{c+f}(t) = \int_{\partial_c \Omega} \left[\Gamma_{\boldsymbol{\nu}} \dot{d}_{\boldsymbol{\nu}} + \mathbf{\Gamma}_{\boldsymbol{\tau}} . \overset{o}{\mathbf{d}}_{\boldsymbol{\tau}} \right] \tag{3}$$

The frictional contact phenomenon is modelled by combining the normal unilateral contact law and the tangential frictional Coulomb law with *variable* pressure [19]. These multivalued relations depend on the gap distance $d_{\boldsymbol{\nu}}$, the contact velocity $\overset{o}{\mathbf{d}}_{\boldsymbol{\tau}}$ and the frictional stress $\mathbf{\Gamma}$ (split into a normal contact pressure $\Gamma_{\boldsymbol{\nu}}$ and a tangential part $\mathbf{\Gamma}_{\boldsymbol{\tau}}$); they can be written as follows:

$$\text{contact law: } \begin{cases} d_{\boldsymbol{\nu}} \geq 0, \\ \Gamma_{\boldsymbol{\nu}} \leq 0, \\ d_{\boldsymbol{\nu}} \Gamma_{\boldsymbol{\nu}} = 0. \end{cases} \qquad \text{frictional law: } \begin{cases} \overset{o}{\mathbf{d}}_{\boldsymbol{\tau}} = \| \overset{o}{\mathbf{d}}_{\boldsymbol{\tau}} \| \frac{\mathbf{\Gamma}_{\boldsymbol{\tau}}}{\|\mathbf{\Gamma}_{\boldsymbol{\tau}}\|}, \\ \|\mathbf{\Gamma}_{\boldsymbol{\tau}}\| + \mu \Gamma_{\boldsymbol{\nu}} \leq 0, \\ \| \overset{o}{\mathbf{d}}_{\boldsymbol{\tau}} \| (\|\mathbf{\Gamma}_{\boldsymbol{\tau}}\| + \mu \Gamma_{\boldsymbol{\nu}}) = 0. \end{cases} \tag{4}$$

where $\boldsymbol{\nu}$ and $\boldsymbol{\tau}$ are the normal and tangent contact unit vectors on $\partial_c\Omega$; μ is the friction coefficient. For a definition of the quantities $d_{\boldsymbol{\nu}}$ and $\overset{o}{\mathbf{d}}_{\boldsymbol{\tau}}$ in the framework of large deformations, we can refer to [7]. These tribological laws can be written in the form of subdifferential inclusions which derive from conjugate non differentiable convex potentials (in the sense of the subgradient [19]),

$$\Gamma_{\boldsymbol{\nu}} \in \partial\Psi_{\mathbb{R}^+}(d_{\boldsymbol{\nu}}) \quad \text{and} \quad \boldsymbol{\Gamma}_{\boldsymbol{\tau}} \in \partial\Psi^*_{C[\Gamma_{\boldsymbol{\nu}}]}(\overset{o}{\mathbf{d}}_{\boldsymbol{\tau}}), \tag{5}$$

where $\partial\Psi_{\mathbb{R}^+}$ and $\partial\Psi^*_{C[\Gamma_{\boldsymbol{\nu}}]}$ denote, respectively, the subdifferential of the indicator function $\Psi_{\mathbb{R}^+}$ of the positive half-line $\mathbb{R}$ and the subdifferential of Fenchel conjuguated of the indicator function $\Psi^*_{C[\Gamma_{\boldsymbol{\nu}}]}$ of $C[\Gamma_{\boldsymbol{\nu}}]$. $C[\Gamma_{\boldsymbol{\nu}}]$ denotes the convex disk of radius $-\mu\Gamma_{\boldsymbol{\nu}}$. We can note that this convex disk depends on the unknown normal contact stress $\Gamma_{\boldsymbol{\nu}}$.

Nevertheless, in order to obtain energy conservation properties and in the absence of external forces, the work of normal contact reactions at time t must vanished [13]:

$$\mathcal{W}_c = \int_{\partial_c\Omega} \dot{d}_{\boldsymbol{\nu}}\Gamma_{\boldsymbol{\nu}} = 0 \tag{6}$$

So for energy conservation purpose, the following persistent condition [13, 4] has to be added,

$$\text{persistent condition:} \quad \dot{d}_{\boldsymbol{\nu}}\Gamma_{\boldsymbol{\nu}} = 0 \tag{7}$$

This condition means that normal contact reactions can only appear during persistent contact. One can easily prove [12] that the addition of the persistent condition (7) to the unilateral contact law gives the following conditions:

$$\begin{cases} \text{if} \;\; d_{\boldsymbol{\nu}} > 0 \quad \Gamma_{\boldsymbol{\nu}} = 0 \\ \text{if} \;\; d_{\boldsymbol{\nu}} = 0 \quad \Gamma_{\boldsymbol{\nu}} \in \partial\Psi_{\mathbb{R}^+}(\dot{d}_{\boldsymbol{\nu}}) \end{cases} \tag{8}$$

2.2 Usual energy conserving frameworks

In order to solve the problem (2), we have to use a time integration scheme. When one considers non linear dynamic problems, the standard implicit schemes (θ-method, Newmark schemes, midpoint or HHT methods, see for example [10, 11, 12] ...) lose their unconditional stability. So we have to use implicit energy conservative schemes [20, 8, 5, 12, 16] which are appropriate due to their long term time integration accuracy and stability. These methods are based on the satisfaction of discrete mechanical conservation properties. In the following, we consider a collection of discrete times $(t_p)_{p=1..P}$ which define a partition of the time interval $[0;T] = \bigcup_{p=1}^{P}[t_p; t_{p+1}]$ with $t_{p+1} = t_p + \Delta t$ and $\Delta t = \frac{T}{P}$. By using a second order time integration scheme (midpoint scheme) with energy conservation properties [20, 8, 16], the weak form (2) integrated between the times t_p and t_{p+1}

gives the following system,

$$\begin{cases} \text{Find } \mathbf{u}_{p+1} \in U_0 \quad \text{such that} \\ \frac{1}{\Delta t}\int_\Omega \rho(\dot{\mathbf{u}}_{p+1}-\dot{\mathbf{u}}_p).\mathbf{v} + \int_\Omega \mathbf{\Pi}_{algo} : \nabla \mathbf{v} - \int_\Omega \mathbf{f}_{p+\frac{1}{2}}.\mathbf{v} - \int_{\partial_q\Omega} \mathbf{g}_{p+\frac{1}{2}}.\mathbf{v} \\ \qquad\qquad + \frac{1}{\Delta t}\int_{t_p}^{t_{p+1}} \mathcal{P}_{c+f}(t)dt = 0 \end{cases} \tag{9}$$

where we choose to enforce the frictional contact conditions at the time t_{p+1}, i.e. the dicrete versions of the unilateral contact law ($\Gamma_{\boldsymbol{\nu}_{p+1}} \in \partial\Psi_{\mathbb{R}^+}(d_{\boldsymbol{\nu}_{p+1}})$), of the Coulomb frictional law ($\mathbf{\Gamma}_{\boldsymbol{\tau}_{p+1}} \in \partial\Psi^*_{C[\Gamma_{\boldsymbol{\nu}_{p+1}}]}(\delta \overset{o}{\mathbf{d}}_{\boldsymbol{\tau}_{p+1}})$) but also of the persistent condition ($\Gamma_{\boldsymbol{\nu}_{p+1}}\delta\dot{d}_{\boldsymbol{\nu}_{p+1}} = 0$). In the sytem (9), $\square_{p+\frac{1}{2}} = \frac{1}{2}(\square_p + \square_{p+1})$ and $\square_p$ denotes the approximation of $\square(t_p)$. $\delta\square$ represents the incremental discretization of $\square$. Moreover, the midpoint scheme gives the following relation,

$$\dot{\mathbf{u}}_{p+1} = -\dot{\mathbf{u}}_p + \frac{2}{\Delta t}(\mathbf{u}_{p+1} - \mathbf{u}_p).$$

The time integration scheme (9) used in this work, is characterized by the tensor $\mathbf{\Pi}_{algo}$ proposed by Gonzalez [8] and defined by

$$\begin{cases} \mathbf{\Pi}_{algo} = \mathbf{F}_{p+\frac{1}{2}}\mathbf{\Sigma}_{algo}, \\ \mathbf{\Sigma}_{algo} = 2\frac{\partial W}{\partial \mathbf{C}}(\mathbf{C}_{p+\frac{1}{2}}) + 2[W(\mathbf{C}_{p+1}) - W(\mathbf{C}_p) \\ \qquad\qquad - \frac{\partial W}{\partial \mathbf{C}}(\mathbf{C}_{p+\frac{1}{2}}) : \Delta\mathbf{C}_p]\frac{\Delta\mathbf{C}_p}{\Delta\mathbf{C}_p:\Delta\mathbf{C}_p}, \end{cases} \tag{10}$$

with $\Delta\mathbf{C}_p = \mathbf{C}_{p+1} - \mathbf{C}_p$. The previous relations (10) were introduced in order to ensure exact energy conservation characterized by the following condition,

$$\mathbf{\Pi}_{algo} : (\nabla\mathbf{u}_{p+1} - \nabla\mathbf{u}_p) = W(\mathbf{C}_{p+1}) - W(\mathbf{C}_p) \quad \text{with} \quad \mathbf{C}_{p+1} = \mathbf{F}^t_{p+1}\mathbf{F}_{p+1}.$$

Furthermore, many works have been devoted to extend these conservative formulations to frictionless impact; more precisely, Laursen and Chawla [13] and Amero and Petocz [4] have shown the interest of the persistency condition to conserve the energy in the discrete framework. But these works are characterized by a contact interpenetration that only can vanished when the time step tends towards zero. Recently, in order to overcome this drawback Laursen and Love [14] have developed an efficient method by introducing a discrete jump in velocity. Furthermore, Hauret [9] has considered a specific penalized enforcement of the contact conditions which permits implicitly to ensure the persistent condition.

2.3 Adaptation to impact problems

In this section, we present an energy-conserving algorithm for hyperelastodynamic contact problems which differs from the approaches mentionned above ([14] and [9]) and also permits to ensure both the Kuhn-Tucker and persistency conditions at the end of each time step.

With an aim of taking into account the contact at the time t_{p+1}, we approximate the frictional contact term $\int_{t_p}^{t_p+1} \mathcal{P}_{c+f}(t)dt$ by

$$\int_{t_p}^{t_p+1} \mathcal{P}_{c+f}(t)dt \approx \Delta t \left(\int_{\partial_c \Omega} [\Gamma_{\boldsymbol{\nu}_{p+1}} \delta \dot{d}_{\boldsymbol{\nu}_{p+1}} + \boldsymbol{\Gamma}_{\boldsymbol{\tau}_{p+1}} . \delta \overset{o}{\mathbf{d}}_{\boldsymbol{\tau}_{p+1}}] \right) \tag{11}$$

Furthermore, we choose to enforce at each time increment the unilateral contact law ($\Gamma_{\boldsymbol{\nu}_{p+1}} \in \partial \Psi_{\mathbb{R}^+}(d_{\boldsymbol{\nu}_{p+1}})$) and also the persistent condition ($\delta \dot{d}_{\boldsymbol{\nu}_{p+1}} \Gamma_{\boldsymbol{\nu}_{p+1}} = 0$). Indeed, the fact of adding these two laws permits to ensure the conditions (8) at the time t_{p+1}. To do that, we developed an extended Newton method which can be decomposed in two steps, a preliminary step (a) in which we solve the system (9) with the frictional contact law (4) and a final step (b) in which we use the law (8) and the associated frictional Coulomb law. This extended strategy can be written as follows:

step (a): Newton scheme to solve the system (9)

$$\text{with} \quad \begin{cases} \Gamma_{\boldsymbol{\nu}_{p+1}} \in \partial \Psi_{\mathbb{R}^+}(d_{\boldsymbol{\nu}_{p+1}}) \\ \boldsymbol{\Gamma}_{\boldsymbol{\tau}_{p+1}} \in \partial \Psi^*_{C[\Gamma_{\boldsymbol{\nu}_{p+1}}]}(\delta \overset{o}{\mathbf{d}}_{\boldsymbol{\tau}_{p+1}}) \end{cases}$$

step (b): Newton scheme to solve the system (9)

$$\text{with} \quad \begin{cases} \text{if} \;\; d_{\boldsymbol{\nu}_{p+1}} > 0 \quad \Gamma_{\boldsymbol{\nu}_{p+1}} = 0 \\ \text{if} \;\; d_{\boldsymbol{\nu}_{p+1}} = 0 \quad \Gamma_{\boldsymbol{\nu}_{p+1}} \in \partial \Psi_{\mathbb{R}^+}(\delta \dot{d}_{\boldsymbol{\nu}_{p+1}}) \\ \qquad\qquad\qquad\quad \boldsymbol{\Gamma}_{\boldsymbol{\tau}_{p+1}} \in \partial \Psi^*_{C[\Gamma_{\boldsymbol{\nu}_{p+1}}]}(\delta \overset{o}{\mathbf{d}}_{\boldsymbol{\tau}_{p+1}}) \end{cases}$$

This approach allows to cancel some penetrations during impacts which arrive when one solves only the step (b). Once the status of contact was found (step (a)), we apply then the persistent conditions (8) which will restore the conservation of energy without disturbing too much the state of the contact. The drawback of this approach is that it requires to carry out some additional Newton iterations in order to solve the problem of the step (b). In a practical point of view, one notes an overcost from 4 to 6 iterations for the convergence of the step (b).

After a fully discretization step (time and space), we deduce the non linear systems defined by

$$\begin{aligned} \mathcal{R}(\mathbf{u}_{p+1}, \boldsymbol{\lambda}_{p+1}, \tilde{\boldsymbol{\lambda}}_{\boldsymbol{\nu}_{p+1}}) \;=\; & \frac{1}{\Delta t} \mathcal{M}(\dot{\mathbf{u}}_{p+1} - \dot{\mathbf{u}}_p) \;+\; \mathcal{G}_{algo}(\mathbf{u}_{p+1}, \mathbf{u}_p) \\ & + \mathcal{F}(\mathbf{u}_{p+1}, \boldsymbol{\lambda}_{p+1}) \;-\; \mathbf{q}_{p+\frac{1}{2}} = \mathbf{0} \end{aligned} \tag{12}$$

where $\mathcal{M}$ comes from the discretization of the inertia term $\frac{1}{\Delta t} \int_\Omega \rho(\dot{\mathbf{u}}_{p+1} - \dot{\mathbf{u}}_p).\mathbf{v}$ and $\mathcal{G}_{algo}$ is due to the discretization of the hyperelastic part $\int_\Omega \boldsymbol{\Pi}_{algo} : \nabla \mathbf{v}$ and $\mathbf{q}_{p+\frac{1}{2}}$ comes from the discretization of the external forces $\int_\Omega \mathbf{f}.\mathbf{v} + \int_{\partial_g \Omega} \mathbf{g}.\mathbf{v}$. We note $\mathcal{F}(\mathbf{u}_{p+1}, \boldsymbol{\lambda}_{p+1})$ the discretization of the frictional contact operator obtained by using a quasi-Lagrangean formulation which permits to treat in an exact way

the frictional contact laws (step (a)) but also the persistent frictional contact conditions (step (b)). This formulation is characterized by the lagrangean multiplier $\boldsymbol{\lambda}$ which permits to enforce respectively the steps (a) and (b). During the step (a) the multiplier $\boldsymbol{\lambda}$ takes the value $\hat{\boldsymbol{\lambda}} = (\hat{\lambda}_{\boldsymbol{\nu}}\boldsymbol{\nu}, \hat{\boldsymbol{\lambda}}_{\boldsymbol{\tau}})$ which is in relation with the frictional contact law (4). In addition, during the step (b) $\boldsymbol{\lambda}$ takes the value $\tilde{\boldsymbol{\lambda}} = (\tilde{\lambda}_{\boldsymbol{\nu}}\boldsymbol{\nu}, \tilde{\boldsymbol{\lambda}}_{\boldsymbol{\tau}})$ which is dedicated to the frictional persistent conditions. The operators $\mathcal{R}$ and $\mathcal{F}$ can take respectively the form $\mathcal{R}^a$ or $\mathcal{R}^b$ and $\mathcal{F}^a$ or $\mathcal{F}^b$ according the step (a) or (b).The forms of the operator $\mathcal{F}$ are the following (we remove the indices $p+1$ with an aim of reducing the writing):

$$\begin{aligned}
&\text{step } (a) \quad \mathcal{F}^a(\mathbf{u}, \hat{\boldsymbol{\lambda}}) = \begin{pmatrix} \nabla_{\mathbf{u}} \hat{l}^r_{\boldsymbol{\nu}}(\mathbf{u}, \hat{\lambda}_{\boldsymbol{\nu}}) + \nabla_{\mathbf{u}} \hat{l}^r_{\boldsymbol{\tau}}(\mathbf{u}, \hat{\boldsymbol{\lambda}}_{\boldsymbol{\tau}}; \Gamma_{\boldsymbol{\nu}}) \\ \nabla_{\hat{\boldsymbol{\lambda}}} \hat{l}^r_{\boldsymbol{\nu}}(\mathbf{u}, \hat{\lambda}_{\boldsymbol{\nu}}) + \nabla_{\hat{\boldsymbol{\lambda}}} \hat{l}^r_{\boldsymbol{\tau}}(\mathbf{u}, \hat{\boldsymbol{\lambda}}_{\boldsymbol{\tau}}; \Gamma_{\boldsymbol{\nu}}) \end{pmatrix}, \\
&\text{step } (b) \quad \text{if } d_{\boldsymbol{\nu}} = 0 \quad \mathcal{F}^b(\mathbf{u}, \tilde{\boldsymbol{\lambda}}) = \begin{pmatrix} \nabla_{\mathbf{u}} \tilde{l}^r_{\boldsymbol{\nu}}(\mathbf{u}, \tilde{\lambda}_{\boldsymbol{\nu}}) + \nabla_{\mathbf{u}} \tilde{l}^r_{\boldsymbol{\tau}}(\mathbf{u}, \tilde{\boldsymbol{\lambda}}_{\boldsymbol{\tau}}; \Gamma_{\boldsymbol{\nu}}) \\ \nabla_{\tilde{\boldsymbol{\lambda}}} \tilde{l}^r_{\boldsymbol{\nu}}(\mathbf{u}, \tilde{\lambda}_{\boldsymbol{\nu}}) + \nabla_{\tilde{\boldsymbol{\lambda}}} \tilde{l}^r_{\boldsymbol{\tau}}(\mathbf{u}, \tilde{\boldsymbol{\lambda}}_{\boldsymbol{\tau}}; \Gamma_{\boldsymbol{\nu}}) \end{pmatrix}, \\
&\qquad\qquad \text{if } d_{\boldsymbol{\nu}} > 0 \quad \mathcal{F}^b(\mathbf{u}, \tilde{\boldsymbol{\lambda}}) = 0.
\end{aligned}$$

The terms $\hat{l}^r_{\boldsymbol{\nu}}$, $\tilde{l}^r_{\boldsymbol{\nu}}$, $\hat{l}^r_{\boldsymbol{\tau}}$ and $\tilde{l}^r_{\boldsymbol{\tau}}$ represent respectively the regularization of the functions $\Psi_{\mathbb{R}^+}(d_{\boldsymbol{\nu}})$, $\Psi_{\mathbb{R}^+}(\delta \dot{d}_{\boldsymbol{\nu}})$, $\Psi^*_{\hat{C}}(\delta \overset{o}{\mathbf{d}}_{\boldsymbol{\tau}})$ and $\Psi^*_{\tilde{C}}(\delta \overset{o}{\mathbf{d}}_{\boldsymbol{\tau}})$ and take the following forms,

$$\begin{cases}
\hat{l}^r_{\boldsymbol{\nu}}(\mathbf{v}, \hat{\lambda}_{\boldsymbol{\nu}}) = \left(d_{\boldsymbol{\nu}}(\mathbf{v}), \hat{\lambda}_{\boldsymbol{\nu}}\right) + \frac{r}{2}\|d_{\boldsymbol{\nu}}(\mathbf{v})\|^2 - \frac{1}{2r}\mathrm{dist}^2_{\mathbb{R}^-}\left\{\hat{\lambda}_{\boldsymbol{\nu}} + r d_{\boldsymbol{\nu}}(\mathbf{v})\right\} \\
\tilde{l}^r_{\boldsymbol{\nu}}(\mathbf{v}, \tilde{\lambda}_{\boldsymbol{\nu}}) = \left(\delta \dot{d}_{\boldsymbol{\nu}}(\mathbf{v}), \tilde{\lambda}_{\boldsymbol{\nu}}\right) + \frac{r}{2}\|\delta \dot{d}_{\boldsymbol{\nu}}(\mathbf{v})\|^2 - \frac{1}{2r}\mathrm{dist}^2_{\mathbb{R}^-}\left\{\tilde{\lambda}_{\boldsymbol{\nu}} + r\delta \dot{d}_{\boldsymbol{\nu}}(\mathbf{v})\right\} \\
\hat{l}^r_{\boldsymbol{\tau}}(\mathbf{v}, \hat{\boldsymbol{\lambda}}_{\boldsymbol{\tau}}) = \left(\delta \overset{o}{\mathbf{d}}_{\boldsymbol{\tau}}(\mathbf{v}), \hat{\boldsymbol{\lambda}}_{\boldsymbol{\tau}}\right) + \frac{r}{2}\|\delta \overset{o}{\mathbf{d}}_{\boldsymbol{\tau}}(\mathbf{v})\|^2 - \frac{1}{2r}\mathrm{dist}^2_{\hat{c}}\left\{\hat{\boldsymbol{\lambda}}_{\boldsymbol{\tau}} + r\delta \overset{o}{\mathbf{d}}_{\boldsymbol{\tau}}\right\} \\
\tilde{l}^r_{\boldsymbol{\tau}}(\mathbf{v}, \tilde{\boldsymbol{\lambda}}_{\boldsymbol{\tau}}) = \left(\delta \overset{o}{\mathbf{d}}_{\boldsymbol{\tau}}(\mathbf{v}), \tilde{\boldsymbol{\lambda}}_{\boldsymbol{\tau}}\right) + \frac{r}{2}\|\delta \overset{o}{\mathbf{d}}_{\boldsymbol{\tau}}(\mathbf{v})\|^2 - \frac{1}{2r}\mathrm{dist}^2_{\tilde{c}}\left\{\tilde{\boldsymbol{\lambda}}_{\boldsymbol{\tau}} + r\delta \overset{o}{\mathbf{d}}_{\boldsymbol{\tau}}\right\},
\end{cases} \tag{13}$$

where r is a positive penalty factor; even if the same notation is conserved for the factor r, notice that its value is not the same one for the step (a) and (b). Alart and Curnier [3] have introduced a particular form of the "quasi" Lagrangean by substituting $C[\tau_n]$ by the augmented convex set $\hat{C}$; we introduce a similar form for the augmented convex $\tilde{C}$:

$$\begin{cases}
\hat{C}\left(\hat{\lambda}_{\boldsymbol{\nu}}, d_{\boldsymbol{\nu}}(\mathbf{u})\right) := C[\mathrm{proj}_{\mathbb{R}^-}\left(\hat{\lambda}_{\boldsymbol{\nu}} + r d_{\boldsymbol{\nu}}(\mathbf{u})\right)], \\
\tilde{C}\left(\tilde{\lambda}_{\boldsymbol{\nu}}, \delta \dot{d}_{\boldsymbol{\nu}}(\mathbf{u})\right) := C[\mathrm{proj}_{\mathbb{R}^-}\left(\tilde{\lambda}_{\boldsymbol{\nu}} + r\delta \dot{d}_{\boldsymbol{\nu}}(\mathbf{u})\right)].
\end{cases}$$

Moreover, this approach of "quasi" augmented Lagrangean permits to satisfy exactly the contact constraints and friction criteria contrary to penalty techniques [21]. For more details about the quasi-Lagrangean formulation see [3]. At each time increment the non linear system (12) can be solved by a generalized Newton method developed in [3]. This method leads to the following iterative linearization scheme (indexed by i),

$$\mathbf{x}_{i+1,p+1} = \mathbf{x}_{i,p+1} - \left(\partial_{\mathbf{x}_{p+1}} \mathcal{R}(\mathbf{x}_{i,p+1})\right)^{-1} \mathcal{R}(\mathbf{x}_{i,p+1}), \tag{14}$$

where the variable $\mathbf{x}_{i+1,p+1}$ denotes the pair $(\mathbf{u}_{i+1,p+1}, \boldsymbol{\lambda}_{i+1,p+1})$. Through this Newton method, we choose to treat both variables $\mathbf{u}_{p+1}$ and $\boldsymbol{\lambda}_{p+1}$ simultaneously. So we can formulate the system (14) by the solution of a linear system:

$$\begin{aligned}\mathcal{K}_{i,p+1}\Delta\mathbf{x}_{i,p+1} = -\frac{1}{\Delta t}\mathcal{M}(\dot{\mathbf{u}}_{i,p+1} - \dot{\mathbf{u}}_p) - \mathcal{G}_{algo}(\mathbf{u}_{i,p+1}, \mathbf{u}_p) \\ - \mathcal{F}(\mathbf{u}_{i,p+1}, \boldsymbol{\lambda}_{i,p+1}) + \mathbf{q}_{p+\frac{1}{2}} \qquad (15)\end{aligned}$$

$$\text{with} \quad \mathcal{K}_{i,p+1} = \frac{2}{\Delta t^2}\mathbf{M} + \mathbf{K}^e_{i,p+1} + \mathbf{K}^c_{i,p+1}$$

$$\text{and} \quad \Delta\mathbf{x}_{i,p+1} = (\mathbf{u}_{i+1,p+1} - \mathbf{u}_{i,p+1}, \boldsymbol{\lambda}_{i+1,p+1} - \boldsymbol{\lambda}_{i,p+1})$$

where $\mathbf{M} = \partial_{\dot{\mathbf{u}}_{p+1}}\mathcal{M}$ represents the mass matrix and $\mathbf{K}^e_{i,p+1} = \partial_{\mathbf{u}_{p+1}}\mathcal{G}_{algo}$ the hyperelastic tangent matrix and $\mathbf{K}^c_{i,p+1} = \partial_{\mathbf{x}_{p+1}}\mathcal{F}(\mathbf{x}_{i,p+1})$ denotes the frictional contact tangent matrix. We can insist on the fact that the matrix $\mathcal{K}_{i,p+1}$ of system (15) is strongly non symmetric. The non symmetries come from the friction law but also from the mathematical form of tensor $\boldsymbol{\Pi}_{algo}$ (see [8]). So we resume the adapted numerical scheme used by the following algorithm,

for $p = 0$ ..
- $\mathbf{x}_{0,p+1} = \mathbf{x}_p$
- $\dot{\mathbf{u}}_{0,p+1} = -\dot{\mathbf{u}}_p$
- step (a): for $i = 0$ ..
  - $\mathcal{K}_{i,p+1}\Delta\mathbf{x}_{i,p+1} = -\mathcal{R}^a(\mathbf{x}_{i,p+1})$
  - $\mathbf{x}_{i+1,p+1} = \mathbf{x}_{i,p+1} + \Delta\mathbf{x}_{i,p+1}$
  - $\dot{\mathbf{u}}_{i+1,p+1} = \dot{\mathbf{u}}_{i,p+1} + \frac{2}{\Delta t}\Delta\mathbf{u}_{i,p+1}$
  - until convergence $\quad (i \leftarrow i+1) \quad \rightsquigarrow i^a$
- step (b): for $i = i^a$ ..
  - $\mathcal{K}_{i,p+1}\Delta\mathbf{x}_{i,p+1} = -\mathcal{R}^b(\mathbf{x}_{i,p+1})$
  - $\mathbf{x}_{i+1,p+1} = \mathbf{x}_{i,p+1} + \Delta\mathbf{x}_{i,p+1}$
  - $\dot{\mathbf{u}}_{i+1,p+1} = \dot{\mathbf{u}}_{i,p+1} + \frac{2}{\Delta t}\Delta\mathbf{u}_{i,p+1}$
  - until convergence $\quad (i \leftarrow i+1)$

until p = P $\quad (p \leftarrow p+1)$

Notice that i^a represents the iteration number necessary to obtain the convergence of the step (a).

2.4 Two numerical simulations

In this section, we present two numerical simulations in order to analyse and to compare the behaviour of some classical time integration schemes (trapezoidal

rule, midpoint rule and HHT scheme, ...) with the algorithm presented in this paper. The first application (section 2.4.1) concerns an academic hyperelastodynamic problem: the cantilever beam. The interest of this application is only to recall the numerical behaviour of several time integration schemes to solve non linear dynamic problem without contact and friction. The second application (section 2.4.2) represents the bounces of the ring against a rigid surface. This representative simulation [12] permits to assess the performance and also to underscore the conservative behaviour of the proposed method.

2.4.1 A non linear elastodynamic problem : a cantilever beam

We consider an elastic beam clamped on one of its tips and an external time independent loading g on the opposite tip. The compressible material response

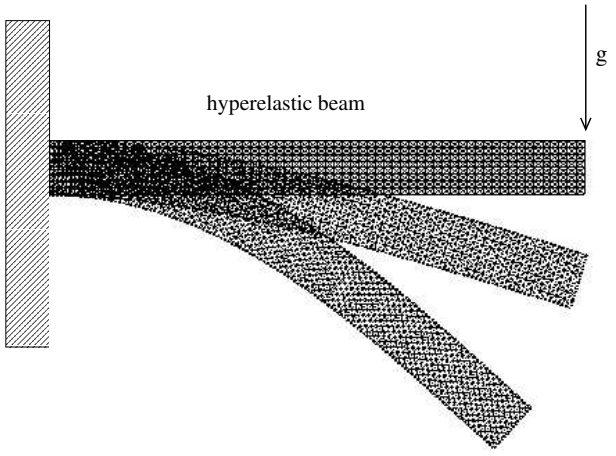

Figure 1: Deformed sequence of a cantilever beam.

considered is governed by an Ogden constitutive law defined by

$$W(\mathbf{C}) = c_1(I_1 - 3) + c_2(I_2 - 3) + a(I_3 - 1) - (c_1 + 2c_2 + a)\ln I_3,$$

where I_1, I_2 and I_3 represent the three invariants of the tensor $\mathbf{C}$.

The mesh and its deformed configurations during the time are presented in figure 1. The material properties and dimensions of the ring are as follows : material constants $c_1 = 0.5MPa, c_2 = 0.5 * 10^{-2}MPa, a = 0.35MPa$, density $\rho = 1000kg/m^3$, length of the beam $L = 10m$ and width of the beam $l = 1m$. Moreover, we consider the final time $T = 10s$ and a time step $\Delta t = 0.1s$.

In the following, we recall some classical results in respect to various time integration schemes that we can find for example in [9]. In the figure (2), we

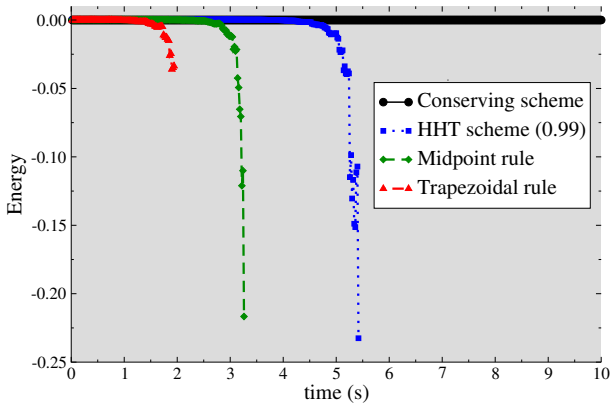

Figure 2: Discrete energy of the dynamic cantilever system.

give the evolution the discrete energy of the dynamic system according several algorithms as the Gonzalez conserving scheme, the HHT scheme, the midpoint and trapezoidal rule. We can note that only the Gonzalez scheme is exactly conservative. For the other schemes, energy blow up is observed; the worst energy conservation holds for the trapezoidal rule. This drawback can be avoided by adopting a small time step, but a realistic control of discrete energy by the time step is hard to obtain and moreover the computational cost becomes higher.

2.4.2 A dynamic frictional contact problem : bounces of a ring against rigid surface

We consider now the bounces of an elastic ring against a rigid surface. In this case, the non linearities come from the friction contact laws but also from the hyperelastic law of the material (we take the same law as in the previous application (section 2.4.1)).

The elastic ring is thrown with an initial velocity at a 45^o angle to a flat rigid surface as depicted in figure 3. The material properties and dimensions of the ring are as follows: material constants $c_1 = 0.5MPa, c_2 = 0.5 * 10^{-2}MPa, a = 0.35MPa$, outer radius of the ring $r_0 = 1m$, inner radius $= 0.9m$, density $\rho = 1000kg/m^3$. Moreover, we consider the final time $T = 100s$ and a time step $\Delta t = 0.1s$.

As in the previous example (section 2.4.1), we present in the figure (4) the evolution of the discrete energy of the dynamic system in respect to various time integration schemes and we focus our attention on the method presented in section (2.3). To analyse the behaviour of our method, we consider three simulations:

- the curve (●) represents our method to solve the considered problem with contact and friction,

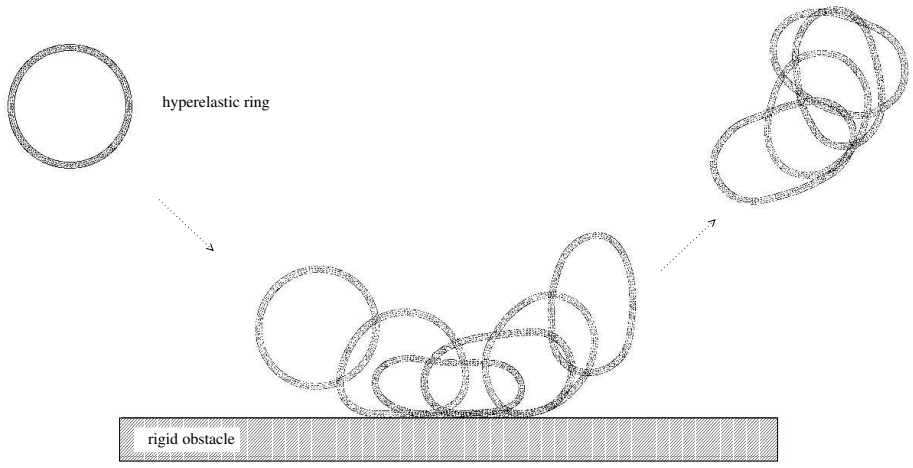

Figure 3: Deformed sequence of the hyperelastic ring during and after the first impact.

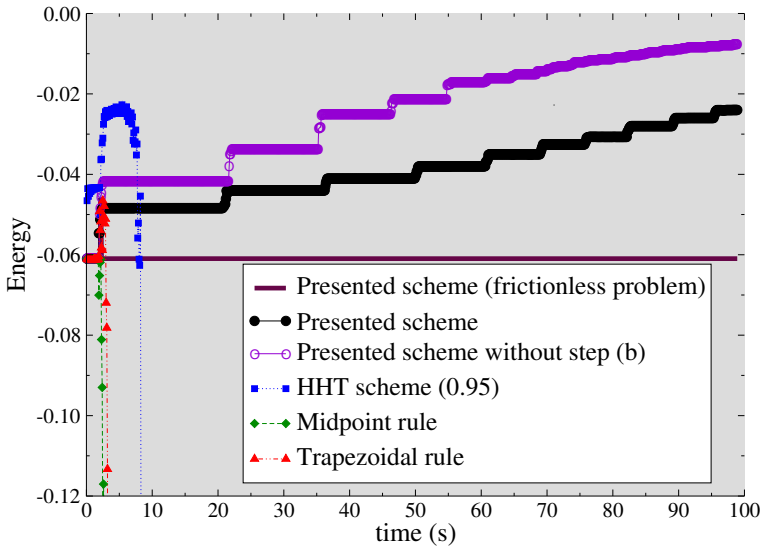

Figure 4: Discrete energy of the ring bounces problem.

- the curve ($\ominus$) denotes our method to solve the same problem but without friction,

- a variant of the method in which we use only the step (a) (without the

step (b)) to solve the problem with contact and friction (curve $(-)$).
Firstly, we can note that after the first impact (time $t = 2.5$), the methods (curve $\blacktriangleleft$, $\blacksquare$ and $\blacklozenge$) not using the Gonzalez form of Π_{algo} (10), are characterized by a energy blow up. In an other hand, the proposed scheme enables a long term time integration with a perfect energy conservation in the case we consider the problem without friction (curve $(\ominus)$). In the case we solve the problem with contact and friction, our method (curve $(\bullet)$) makes it possible to dissipate energy reasonably with an admissible frictional dissipation phenomenon. But if we consider only the step (a) to solve the problem (curve $(-)$), the dissipation becomes physically nonrealistic because in this case the unilateral condition also induces a dissipation.

3 Scalable domain decomposition methods

We make a point of specifing that the presentation of the work related to this part (section 3) is based on results presented in [6].

3.1 The usual Balancing method

The linear systems (15) can be solved by a domain decomposition method [15] which has to be adapted to the non symmetry but also to the presence of inertia terms. Before giving the adaptations to non linear dynamic problems, we present briefly in this section the principal features of a scalable nonoverlapping domain decomposition method : the Balancing method [18, 15]. We choose to adopt a primal Schur complement method written with displacement variables. The basic idea in nonoverlapping domain decomposition methods is to split the domain Ω of study into N small nonoverlapping subdomains $\Omega^n (n = 1, N)$ and interfaces $\Gamma^n (n = 1, N)$ defined by :

$$\Omega = \bigcup_{n=1}^{N} \Omega^n \quad \text{with} \quad \Gamma^n = \partial\Omega^n \cap \left(\bigcup_{\substack{p=1 \\ p \neq n}}^{N} \partial\Omega^p \right) - \partial\Omega.$$

Substructuring techniques consist then in reducing the original global system to an interface problem by a block Gaussian elimination of the internal degrees of freedom and in iteratively solving the resulting variational interface problem :

$$\exists \bar{\mathbf{u}} \in \bar{V} \ / \ < \mathbf{S}_{i,p+1} \bar{\mathbf{u}}, \bar{\mathbf{v}} > = < \bar{\mathbf{f}}_{i,p+1}, \bar{\mathbf{v}} > \ \forall \bar{\mathbf{v}} \in \bar{V} = tr(V)|_{\Gamma}, \qquad (16)$$

where V is the discrete set defined from the space U_0 and $\Gamma = \bigcup_{n=1}^{N} \Gamma^n$. The matrices $\mathbf{S}_{i,p+1} = \sum_{n=1}^{N} \mathcal{R}^n \mathbf{S}^n_{i,p+1} (\mathcal{R}^n)^t$ denote the global Schur complement matrix defined on Γ; $(\mathcal{R}^n)^t$ is the restriction operator which goes from Γ to Γ^n. The local Schur complement matrices $\mathbf{S}^n_{i,p+1}$ are defined on Γ^n by

$$\mathbf{S}^n_{i,p+1} = \bar{\mathcal{K}}^n_{i,p+1} - (\mathbf{B}^n_{i,p+1})^t (\mathring{\mathcal{K}}^n_{i,p+1})^{-1} \mathbf{B}^n_{i,p+1}.$$

To do that, we have considered the subdomain stiffness matrix formulated by $K^n_{i,p+1} = \begin{pmatrix} \mathring{K}^n_{i,p+1} & \mathbf{B}^n_{i,p+1} \\ (\mathbf{B}^n_{i,p+1})^t & \bar{K}^n_{i,p+1} \end{pmatrix}$. The first block $\mathring{K}^n_{i,p+1}$ corresponds to the internal degrees of freedom in the subdomain Ω^n, the second one $\bar{K}^n_{i,p+1}$ corresponds to the interface degrees of freedom on Γ^n. The matrix $\mathbf{B}^n_{i,p+1}$ represents the contribution connecting Γ^n to Ω. The interface problem (16) can be solved by a preconditioned conjugate gradient method (symmetric cases) or the GMRES method (non symmetric cases). Hereafter, we use the multilevel Neumann-Neumann preconditioner [15, 17]. This iterative technique never requires the explicit calculation of the matrix $\mathbf{S}$. We have just to form the matrix vector products $\mathbf{S}\bar{\mathbf{p}}$ and $\mathbf{M^{-1}}\bar{\mathbf{r}}$ by solving independent auxiliary Dirichlet and Neumann problems on the local subdomains and a global coarse problem defined on a space of singular (rigid body) motions. The adaptation of the Balancing Method [18, 15] to solve linear systems issued from non linear elastodynamic problems can be realized by using the theoritical frameworks of Schwarz additive decomposition method with introduction of a coarse space. It consists in decomposing the interface space $\bar{V}$ into a coarse and a fine component $\bar{V}_G$ and $\bar{V}_f$. For Neumann-Neumann domain decomposition techniques, the coarse space is defined by adding local rigid components $\bar{V}_G = \sum_{n=1}^N D^n Z^n$ with D^n a given partition of unity defined on the interface ($\sum_{n=1}^N D^n R^n = Id|_{\bar{V}}$) and the fine space is defined by orthogonality

$$\bar{V}_f = \{\bar{\mathbf{v}}_f \in \bar{V} = \sum_{n=1}^N D^n \bar{V}^n, \quad < \mathbf{S}\bar{\mathbf{v}}_f, \bar{\mathbf{v}}_G >= 0, \qquad \forall \bar{\mathbf{v}}_G \in \bar{V}_G\}. \tag{17}$$

The key point is the construction of the local spaces Z^n of rigid motions. This construction must, if that is necessary, regularize local Neumann problems but more especially set the constants of the lower energy modes (like rigid body motions) to zero in the solution of local Neumann problems. For more details on the presentation of the Schwarz additive method, we can refer to [15, 17] for symmetric cases and [1, 2] for non symmetric cases.

With finite deformations and dynamic problems, some rigid body motions "of lower energy" cannot be detected in the factorization step of the local tangent matrices of Neumann problems. These drawbacks come on the one hand from the finite deformations modeling and on the other hand from the regularizing contribution of the mass matrix. So we have to introduce a specific detection procedure to construct this lower energy modes especially adapted to non linear dynamic problems. In the following section, we present in detail the construction of the coarse space $\bar{V}_G$ for hyperelastic dynamic problems.

3.2 Adaptations of the two-level Neumann-Neumann preconditioner

The solutions of static and dynamic hyperelastic problems (1) by standard algorithms [10, 8, 16] generate at each increment or time step (subscripted by p) a non linear system (equation (12)) which can be solved by an iterative Newton

method (subscripted by i). According to the reasons mentioned above, we propose an adapted construction of the two level Neumann-Neumann preconditioner based on the following steps

1. Preliminary step : We identify the local degrees of freedom $(P_\alpha^n)_{\alpha=1,m^n}$ which cancel all m^n rigid motions of subdomain n. This detection must be realized during the factorization of the stiffness matrix $(K_0^e)^n$ coming from the linear elastostatic system associated to the non linear elastodynamic problem (12). Notice that we can make arbitrary this dectection, but in this case we don't optimize the size of the coarse system.

2. For each Newton iteration i of each time step p

   (a) We construct the local matrices $\tilde{\mathcal{K}}_{i,p+1}^n$ using the degrees of freedom $(P_\alpha^n)_{\alpha=1,m^n}$ detected in step (1). These regularized matrices are given through the matrices $\mathcal{K}_{i,p+1}^n$ by the following relation:

   $$< \tilde{\mathcal{K}}_{i,p+1}^n \mathbf{v}^n, \mathbf{w}^n >=< \mathcal{K}_{i,p+1}^n \mathbf{v}^n, \mathbf{w}^n > + \sum_{\alpha,\beta} \mathbf{Q}_{\alpha\beta}^n \mathbf{v}^n(P_\alpha^n)\mathbf{w}^n(P_\beta^n), \tag{18}$$

   where $\mathbf{Q}^n$ is a definite positive arbitrary matrix. We can note that in the case of dynamic problems, this construction step can be not realized. Indeed, the matrices $\mathcal{K}_{i,p+1}^n$ of systems (15) are invertible because of the presence of inertia terms (mass matrices); so we take $\tilde{\mathcal{K}}_{i,p+1}^n = \mathcal{K}_{i,p+1}^n$.

   (b) We compute the lower energy modes $(\mathbf{v}_{G\alpha}^n)_{\alpha=1,m^n}$ by solving the regularized Neumann problems set on the space V^n of subdomain displacements functions,

   $$< (\tilde{\mathcal{K}}_{i,p+1}^n)^t \mathbf{v}_{G\alpha}^n, \mathbf{w}^n >= \mathbf{w}^n(P_\alpha^n), \forall \mathbf{w}^n \in V^n, \mathbf{v}_{G\alpha}^n \in V^n. \tag{19}$$

   We can note that we have considered the general non symmetric cases [1, 2]. Indeed, the system (15) is strongly non symmetric due to frictional contact terms but also due to the form of the tensor $\mathbf{\Pi}_{algo}$ (see equation 10).

   (c) We define the local rigid space by $Z^n = \text{vect}\left(\mathbf{v}_{G\alpha}^n, \alpha = 1, m^n\right)$.

For the non linear elastostatic case we replace in the steps (a) and (b) the matrix $\mathcal{K}_{i,p+1}^n$ by the matrix $\mathbf{K}_{i,p+1}^n$. With this construction of lower energy modes, the two-level Neumann-Neumann preconditioner is classically defined for each Newton iteration i by

$$\mathbf{M}_{i,p+1}^{-1}\mathbf{S}_{i,p+1} = \mathbf{P}_G + \sum_{n=1}^{N} (\mathbf{I} - \mathbf{P}_G)\mathbf{D}_{i,p+1}^n (\tilde{\mathbf{S}}_{i,p+1}^n)^{-1} (\mathbf{D}_{i,p+1}^n)^t (\mathbf{I} - \mathbf{P}_G)^t \mathbf{S}_{i,p+1}, \tag{20}$$

where $(\tilde{\mathbf{S}}^n_{i,p+1})^{-1}$ is the regularized Schur inverse matrix and $\mathbf{P}_G$ denotes the orthogonal $\mathbf{S}$-projection of $\bar{V}$ on $\bar{V}_G$ defined by

$$< \mathbf{S}\mathbf{P}_G\bar{\mathbf{v}}, \bar{\mathbf{v}}_G >=< \mathbf{S}\bar{\mathbf{v}}, \bar{\mathbf{v}}_G > \quad \forall \bar{\mathbf{v}}_G \in \bar{V}_G \quad \text{and} \quad \mathbf{P}_G\bar{\mathbf{v}} \in \bar{V}_G. \tag{21}$$

It is important to note that the detection of rigid modes (step(1)) is realized by the linear elasticity matrix $(\mathbf{K}^e_0)^n$. On the other hand, the construction step $(2)-(b)$ is obtained with the regularized matrix $\tilde{\mathcal{K}}^n_{i,p+1}$ or $\mathcal{K}^n_{i,p+1}$ issued from the system (15). By using similar arguments developed in [1, 2], we can note that this choice ensures that the solutions of Neumann problems have all lower energy modes fixed to zero.

The regularized Schur inverse $(\tilde{\mathbf{S}}^n_{i,p+1})^{-1}$ acting on a given linear form L^n defined on the local dual interface space of $\bar{V}^n$ yields the interface vector

$$(\tilde{\mathbf{S}}^n_{i,p+1})^{-1}L^n = Tr(\mathbf{u}^n)_{|\Gamma^n}$$

obtained by solution of the following local (regularized) Neumann problem:

$$< \tilde{\mathcal{K}}^n_{i,p+1}\mathbf{u}^n, \mathbf{w}^n >= L^n(Tr(\mathbf{w}^n)_{|\Gamma^n}), \quad \forall \mathbf{w}^n \in V^n, \mathbf{u}^n \in V^n. \tag{22}$$

This construction ensures that the solution $\mathbf{u}^n = (\tilde{\mathbf{S}}^n_{i,p+1})^{-1}(\mathbf{D}^n_{i,p+1})^t(\mathbf{I}-\mathbf{P}_G)^t\bar{\mathbf{r}}$ have all lower energy modes $\mathbf{u}^n(P^n_\alpha)$ fixed to zero. Indeed, by definition of the modes $\mathbf{v}^n_{G\alpha}$ (equation (19)) and by the construction of $\mathbf{u}^n$ (equation (22)) and by the projection $\mathbf{P}_G$ (equation (21)), we have

$$\mathbf{u}^n(P^n_\alpha) =< (\tilde{\mathcal{K}}^n_{i,p+1})^t\mathbf{v}^n_{G\alpha}, \mathbf{u}^n >=< \bar{\mathbf{r}}, (\mathbf{I}-\mathbf{P}_G)D^n_{i,p+1}\mathbf{v}^n_{G\alpha} >= 0. \tag{23}$$

Moreover, if the regularized procedure (18) is used (for static or quasi-static problems), that does not affect the optimality of the method. Indeed, the relation (23) involves that $< \tilde{\mathcal{K}}^n_{i,p+1}\mathbf{u}^n, \mathbf{u}^n >=< \mathcal{K}^n_{i,p+1}\mathbf{u}^n, \mathbf{u}^n >$.

The numerical results presented in the following section validate this adapted construction of the two-level Neumann-Neumann preconditioner. That permits to find numerical scalable results for non linear elastodynamic problems.

3.3 Two numerical simulations

We take in this section the two numerical applications presented in section 2.4.

3.3.1 A non linear elastodynamic problem : a cantilever beam

The figure 6 gives the evolution of average number of GMRES iterations (per Newton iterations) for a beam decomposed in 2, 5, 10, 20, 40 and 80 subdomains (see figure 5) for a decomposition in 10 subdomains. We observe that the number of iterations obtained with the 2-level Neumann-Neumann preconditioner without adaptations (curve ◀) grows up with respect to the number of subdomains. So the interface solver with this preconditioner loses its classical scalability. We

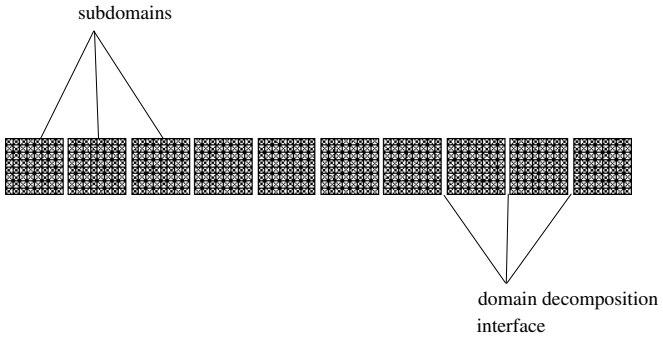

Figure 5: Substructuration of the beam in 10 subdomains.

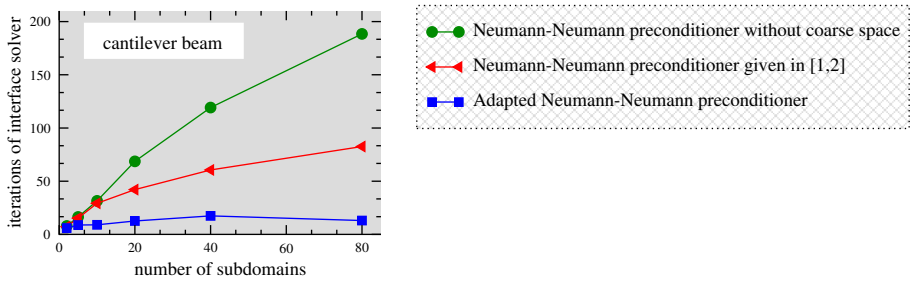

Figure 6: Numerical scalability with Neumann-Neumann preconditioners.

can also remark the inefficiency of the solver using standard Neumann-Neumann preconditioner without coarse space (curve ●). On the other hand, the adapted Neumann-Neumann preconditioner (curve ■) leads to recover the numerical scalability properties i.e. the independence of the solver iterations with respect to the number of subdomains.

3.3.2 A dynamic frictional contact problem : impact of a ring against rigid surface

The figure 8 gives the evolution of average number of GMRES iterations (per Newton iterations) for a ring decomposed in 4, 8, 16, 32, 64 and 128 subdomains (see figure 7 for a decomposition in 32 subdomains). As in the previous example (section 3.3.1), we observe that the 2-level Neumann-Neumann preconditioner without adaptations lose its numerical scalability properties, but on the other hand, the adaptations introduced in section 3.2 make it possible to find these essential properties. Moreover we can remark that the contact and friction laws do not have any effect on the behaviour of the adapted preconditioner.

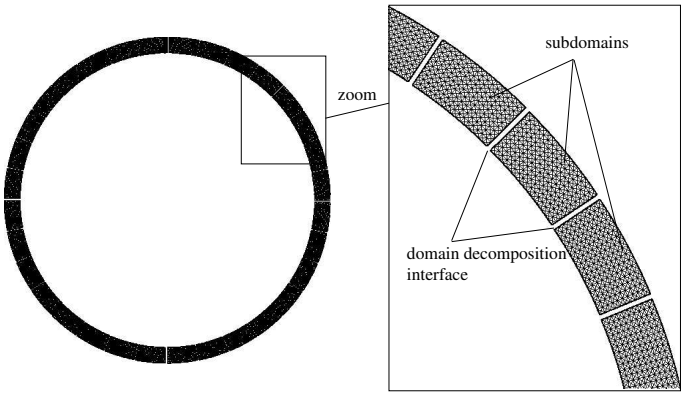

Figure 7: Substructuration of the ring in 32 subdomains.

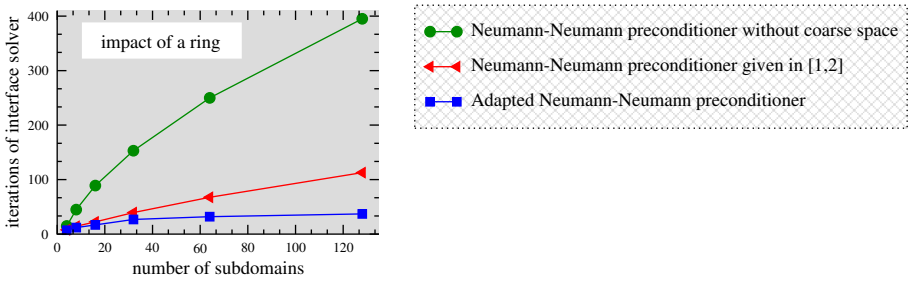

Figure 8: Numerical scalability with Neumann-Neumann preconditioners.

References

[1] P. Alart, M. Barboteu, P. Le Tallec and M. Vidrascu, Méthode de Schwarz additive avec solveur grossier pour problèmes non symétriques. *C. R. Acad. Sci.*, 331(I), pp. 399–404 (2000).

[2] P. Alart, M. Barboteu, P. Le Tallec and M. Vidrascu, An iterative Schwarz method for non symmetric problems. In N. Debit, M. Garbey, R.Hoppe, J. Périaux, D. Keyes and Y. Kuznetsov, editors, *Thirteenth International Conference on Domain Decomposition Method*, http://www.ddm.org, (2000).

[3] P. Alart and A. Curnier, A mixed formulation for frictional contact problems prone to Newton like solution methods. *Comput. Meth. Appl. Mech. Engrg.*, **92**,pp. 353–375 (1991).

[4] F. Armero and E. Petocz, Formulation and analysis of conserving algorithms for frictionless dynamic contact/impact problems. *Comput. Meth. Appl. Mech. Engrg.*, **158**, pp. 269-300 (1998).

[5] F. Armero and I. Romero, On the formulation of high-frequency dissipative time-stepping algorithms for nonlinear dynamics. Part II: second-order methods. *Comput. Meth. Appl. Mech. Engrg.*, **190**, pp. 6783-6824 (2001).

[6] M. Barboteu, An adapted Balancing domain decomposition method for dynamic frictional contact problems in large deformations. *European Congress on Computational Methods in Applied Sciences and Engineering : ECCOMAS*, P. Neittaanmaki, T. Rossi, S. Korotov, E. Onate, J. Periaux and D. Knorzer (eds.), Jyvaskyla (2004).

[7] A. Curnier, Q.C. He and A. Klarbring, Continuum mechanics modelling of large deformation contact with friction. *Contact Mechanics, ed. plenum Press*, (1995).

[8] O. Gonzalez, Exact energy and momentum conserving algorithms for general models in non linear elasticity. *Comput. Meth. Appl. Mech. Engrg.*, **190**, pp. 1763-1783 (2000).

[9] P. Hauret, Numerical methods for the dynamic analysis of two-scale incompressible nonlinear structures, Ph.D. Thesis, Ecole Polytechnique, France (2004).

[10] H. Hilber, T. Hughes and R. Taylor, Improved numerical disspation for time integration algorithms in structural dynamics. *Earth. Engrg. Struc. Dyna.*, **5**, pp. 283-292 (1977).

[11] T. Hughes, *The Finite Element Method, Linear Static and Dynamic Finite Analysis*, Prentice-Hall, (1987).

[12] T.A. Laursen, *Computational contact and impact mechanics*, Springer, (2002).

[13] T. Laursen and V. Chawla, Design of energy conserving algorithms for frictionless dynamic contact problems. *Int. J. Numer. Methods Engrg.*, **40**, pp. 863-886 (1997).

[14] T. Laursen and G. Love Improved implicit integrators for transient impact problems; dynamic frictional dissipation within an admissible conserving framework. *Comput. Meth. Appl. Mech. Engrg.*, **192**, pp. 2223-2248 (2003).

[15] P. Le Tallec, Domain decomposition methods in computational mechanics. *Comput. Mech. Adv.*, **1**, pp. 121-220 (1994).

[16] P. Le Tallec, P. Hauret and A. Rezgui, Efficient solvers for the dynamic analysis of non linear multiscale structures. In H. A. Mang, F. G. Rammerstorfer, J. Eberhardsteiner, Editors, *Fifth World Congress on Computational Mechanics, Vienna, Austria* (July 7-12, 2002).

[17] P. Le Tallec and M. Vidrascu, Generalized Neumann-Neumann Preconditioners for Iterative Substructuring *Proceedings of the ninth international symposium on Domain Decomposition Methods for Partial Differential Equations, Bergen, June 96* pp. 413-425 (1998).

[18] J. Mandel, Balancing domain decomposition. *Communications in Appl. Num. Meth.*, **9**, pp. 233-241 (1993).

[19] J.J. Moreau On unilateral contraints, friction and plasticity. *New Variational Techn. in Math. Phys.*, G. Capriz and G. Stampacchia, CIME II, pp. 175-322 (1973).

[20] J. Simo and N. Tarnow, The discrete energy-momentum method. part I: Conserving algorithms for nonlinear elastodynamics. *ZAMP*, **43**, pp. 757-793 (1992).

[21] P. Wriggers, Computational Contact Mechanics. Wiley-Verlag (2002).

Received: 1 December, 2004

Laboratoire de Mathématiques
et Physique pour les Systèmes(MEPS),
bat. B3, case courrier 12
52, Avenue Paul Alduy
66860 PERPIGNAN cedex, FRANCE
E-mail: barboteu@univ-perp.fr